ACS APPLIED MATERIALS & INTERFACES

Research Article

www.acsami.org

A Cell Apoptosis Probe Based on Fluorogen with Aggregation Induced Emission Characteristics

Qinglian Hu,[†,⊥] Meng Gao,[‡,⊥] Guangxue Feng,[†] Xiaodong Chen,[§] and Bin Liu*[,†,‡]

[†]Department of Chemical and Biomolecular Engineering, National University of Singapore, Singapore 117576, Singapore

[‡]Institute of Materials Research and Engineering (A*STAR), 3 Research Link, Singapore 117602, Singapore

[§]School of Materials Science and Engineering, Nanyang Technological University, 50 Nanyang Avenue, Singapore 639798, Singapore

Supporting Information

ABSTRACT: A fluorogen-based aggregation-induced emission zinc-dipicolylamine (AIE-ZnDPA) probe with aggregation-induced emission characteristics has been designed and synthesized to detect cell apoptosis. AIE-ZnDPA does not respond to healthy cells but selectively stains and lights up fluorescence in the membranes of early stage apoptotic cells as well as the nuclei of late stage apoptotic cells. Without zinc coordination, the precursor lipophilic AIE dipicolylamine (AIE-DPA) probe stains healthy cells and shows high affinity for lipid droplets (LDs).

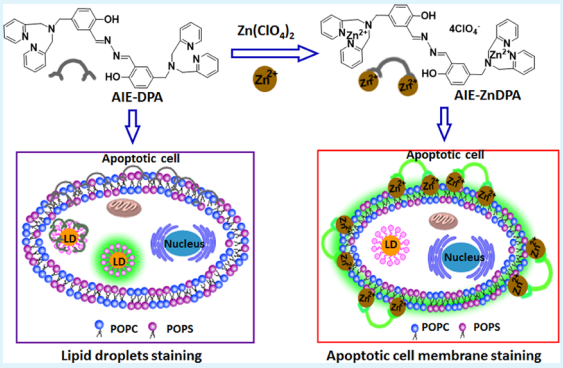

KEYWORDS: *cell apoptosis, zinc coordination, aggregation-induced emission, lipid droplet*

1. INTRODUCTION

Improving the evaluation of cancer cell response to therapeutic drugs is a long-term goal of modern medicine.[1] Apoptosis can provide valuable diagnosis information on therapeutic efficacy.[2,3] Many efforts have been made to develop intracellular methods to elucidate the apoptotic process, such as monitoring of caspase activation,[4,5] laddering of DNA fragmentation,[6,7] and so forth.[8] An attractive extracellular method is to monitor the appearance of phosphatidylserine (PS) on the surface of early apoptotic cells, which occurs prior to DNA fragmentation and plasma membrane permeabilization.[9]

One common approach to target negatively charged PS is to use fluorescent dye-labeled annexin V through in vitro assays.[10,11] Although it has been used extensively, the annexin V probe does not have a very long shelf life. In addition, extracellular Ca^{2+} is needed for complete membrane binding.[12] More recently, fluorescent dyes conjugated with zinc-dipicolylamine (ZnDPA) complexes have been reported as a replacement for annexin V probes to sense PS-rich membranes.[13−16] Most of these dyes with small Stokes shifts show aggregation-caused fluorescence quenching (ACQ) properties. In addition, these probes have intrinsic fluorescence, which makes them unsuitable for continuous monitoring of cell apoptosis. Furthermore, none of these probes have ever been reported to be able to differentiate early and late stages of cell apoptosis.

Recently, several groups have shown interest in developing specific light-up probes based on fluorogens with aggregation-induced emission (AIE) characteristics for sensing and imaging applications.[17−26] AIE fluorogens usually have rotor structures, which have optical properties that are opposite to those of ACQ dyes. Their fluorescence is very weak in dilute solutions but becomes very strong in an aggregated state.[27] Moreover, an excited-state intramolecular proton transfer (ESIPT) mechanism was further introduced to AIE fluorogens, which allowed for the development of light-up probes with sharp imaging contrast, high signal-to-noise ratios, and extremely large Stokes shifts.[28,29]

In this contribution, we report the generation of a small apoptosis probe (AIE-ZnDPA) based on zinc coordination and a salicylaldazine fluorophore skeleton.[30−32] AIE-ZnDPA can anchor to the negatively charged membranes of early stage apoptotic cells to light-up the fluorescence (Scheme 1). When cells undergo late stage apoptosis, AIE-ZnDPA can pass through the cell membrane, enter into nuclei, and interact with nucleic acids to emit bright fluorescence. Moreover, AIE-ZnDPA can also be applied to quantitatively detect real-time imaging of staurosporine (STS)- and hydrogen peroxide (H_2O_2)-induced cell apoptosis. In addition, its precursor, AIE-DPA, which lacks zinc coordination, is able to effectively stain lipid droplets (LDs).

Received: December 15, 2014
Accepted: February 11, 2015
Published: February 11, 2015

DOI: 10.1021/am508838z
ACS Appl. Mater. Interfaces 2015, 7, 4875−4882

Scheme 1. Chemical Structures of AIE-DPA and AIE-ZnDPA, and a Schematic Illustration of AIE-DPA for Intracellular Lipid Droplet Staining and AIE-ZnDPA for the Detection of Cell Apoptosis

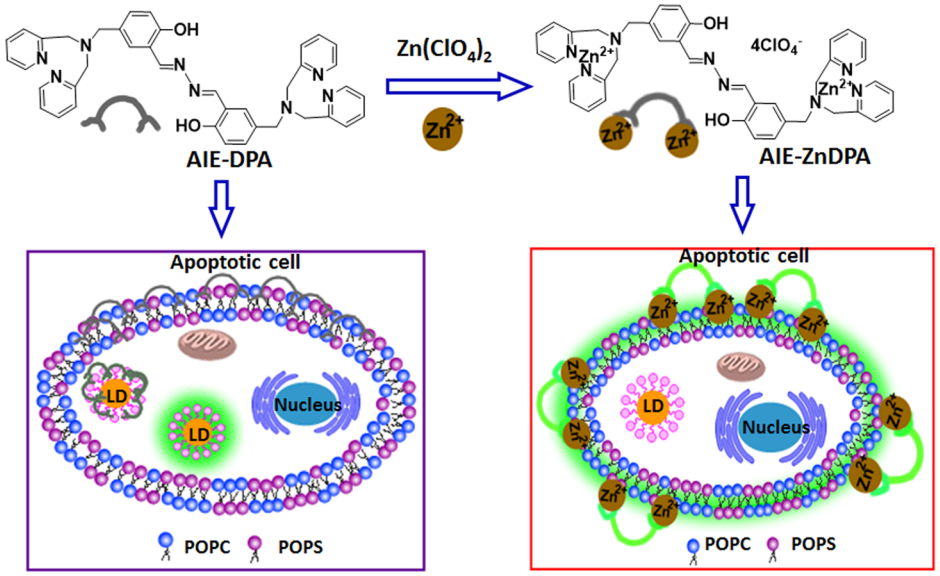

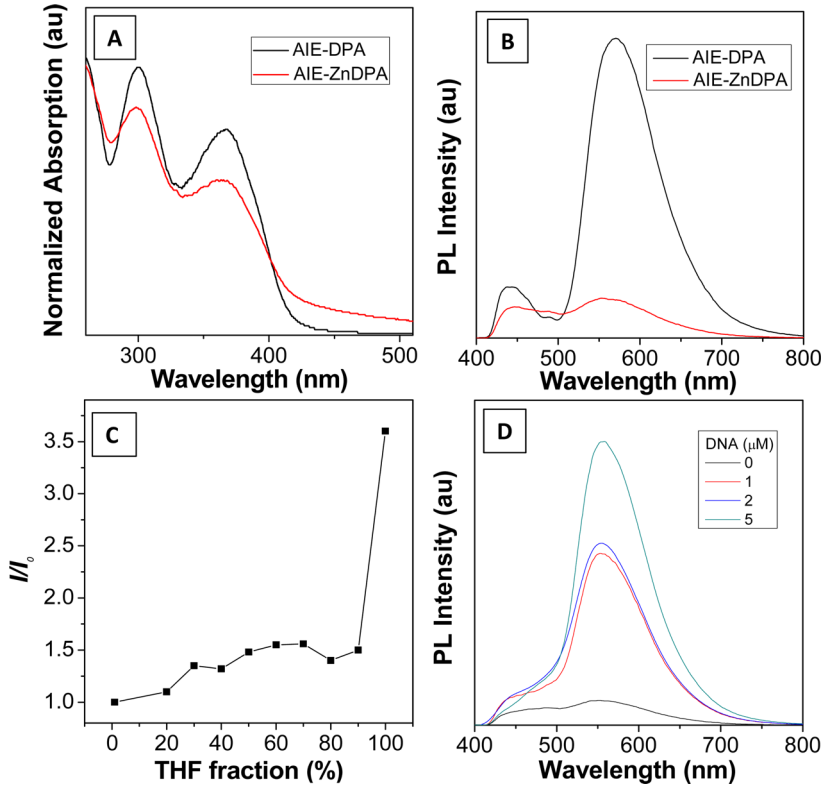

Figure 1. Normalized UV (A) and PL (B) spectra of 10 μM AIE-DPA and AIE-ZnDPA in a DMSO/water mixture (v/v 1:99). (C) Plot of relative PL intensity (I/I_0) at 563 nm versus the solvent composition of the THF/water mixture of AIE-ZnDPA. (D) PL spectra of 10 μM AIE-ZnDPA upon the addition of different concentrations of DNA in water. Ex = 365 nm.

2. RESULTS AND DISCUSSION

The synthetic routes to AIE-DPA and AIE-ZnDPA are shown in Scheme S1 of the Supporting Information. Briefly, the reaction of 5-(chloromethyl)-2-hydroxybenzaldehyde (compound 1) with di(2-picolyl)amine first afforded compound 2 in 85% yield, which was further reacted with hydrazine monohydrate to give product AIE-DPA in 95% yield. AIE-DPA could react with zinc perchlorate hexahydrate to directly afford the desired product of AIE-ZnDPA in a nearly quantitative yield (97%). Their structures were verified by nuclear magnetic resonance (NMR) imaging, Fourier transform infrared (FTIR) spectroscopy, and high-resolution mass spectrometry (Supporting Information, Figures S1−S7).

The UV−vis absorption and photoluminescence (PL) spectra of AIE-DPA and AIE-ZnDPA were measured in aqueous media. As shown in Figure 1A and B, AIE-DPA exists

DOI: 10.1021/am508838z
ACS Appl. Mater. Interfaces 2015, 7, 4875−4882

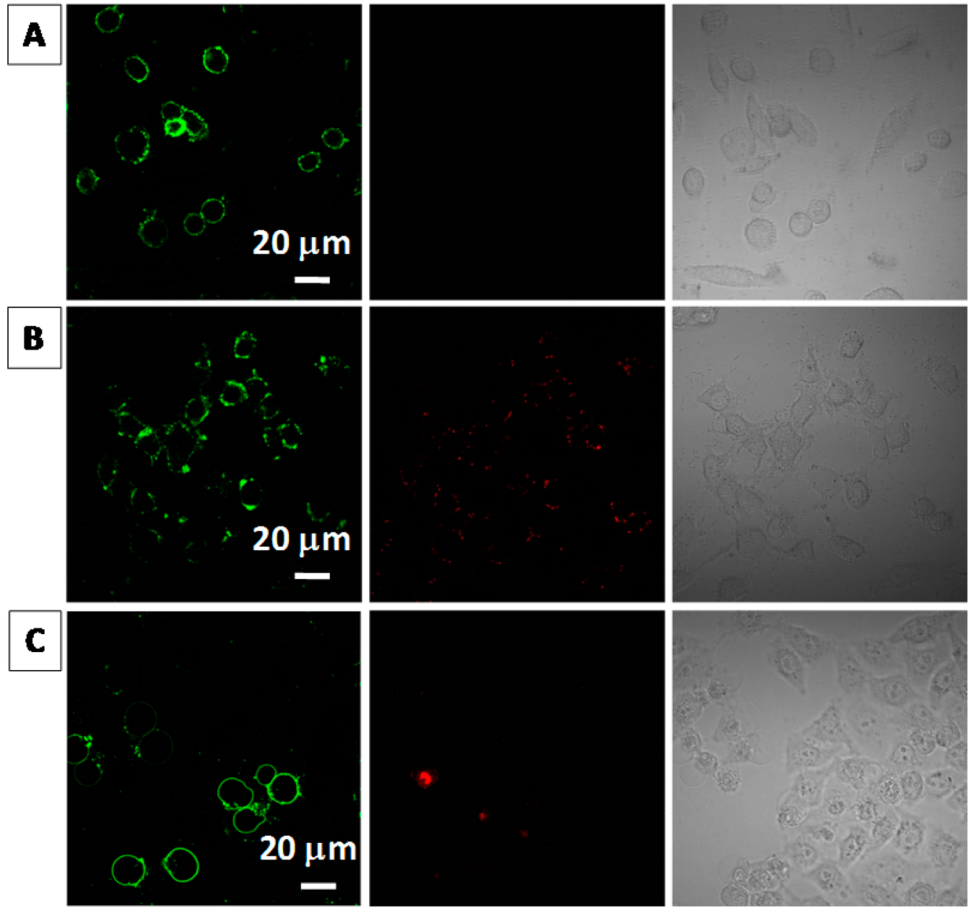

Figure 2. Confocal images of early apoptotic HeLa cells induced by 250 μM H_2O_2 for 6 h (A) or 1 μM staurosporine for 2 h (B), which were followed by incubation with 20 μM AIE-ZnDPA for 30 min at 37 °C and staining with 0.1 μg mL^{-1} propidium iodide for 5 min. (C) HeLa cells were treated with 1 μM staurosporine for 2 h, incubated with Alexa Fluor 488 Annexin V for 30 min at 37 °C, and then stained with 0.1 μg mL^{-1} propidium iodide for 5 min. The red fluorescence originates from propidium iodide. All images share the same scale bar of 20 μm.

in an aggregated state in water, which has an absorption maximum at 365 nm. It has an emission maximum at 555 nm with a fluorescence quantum yield of 2.0 ± 0.2% due to the AIE and ESIPT effects. Upon zinc coordination, AIE-ZnDPA shows weak fluorescence at 555 nm with a quantum yield of less than 0.1% because it is molecularly dispersed in water and has free rotation around the N−N bond, which quenches its fluorescence. For AIE-DPA and AIE-ZnDPA, large Stokes shifts (>190 nm) were observed, which are highly beneficial for bioimaging with minimal self-absorption. The emission of AIE-ZnDPA at 563 nm in water and THF mixtures with different THF fractions is shown in Figure 1C. It shows that low fluorescence is observed in water and that the fluorescence intensity increases significantly when the THF fraction is >80%, showing a typical AIE phenomenon.

To evaluate the potential of AIE-ZnDPA as a fluorescent light-up probe for cell apoptosis imaging, titration experiments were carried out using a mixture of the zwitterionic vesicles 1-palmitoyl-2-oleoyl-*sn*-glycero-3-phosphocholine (POPC) and the anionic vesicles 1-palmitoyl-2-oleoyl-*sn*-glycero-3-phosphoserine (POPS) to mimic the apoptotic cell membrane. Upon excitation at 365 nm, the fluorescence intensity of AIE-ZnDPA in Tris-HCl buffer shows relatively weak fluorescence at ∼483 nm. Upon a 1:1 mixture of POPC/POPS being added to the solution, it exhibited enhanced fluorescence accompanied by a red-shift in the emission maximum from ∼483 to 563 nm due to the ESIPT process. This result indicates that AIE-ZnDPA is able to interact with the negatively charged POPS to light-up its fluorescence (Supporting Information, Figure S8). Changes in the fluorescence spectra of AIE-ZnDPA upon the addition of single-stranded ssDNA (ssDNA: 5′-GGGGGCGGGGGCGG-GGGCGG-3′) were also measured (Figure 1D). As expected, AIE-ZnDPA shows significant fluorescence enhancement with the addition of DNA due to binding-induced restriction of intramolecular motion.

After investigating the optical properties of AIE-ZnDPA in solution, we further explored the potential of the probe for imaging of cell apoptosis. The cytotoxicities of AIE-DPA and AIE-ZnDPA were first evaluated by MTT assays. As shown in Figure S9 in the Supporting Information, after incubating the cells with 10, 20, 40, and 60 μM AIE-DPA or AIE-ZnDPA for 24 h, the cell viabilities are still close to 100%, indicating low cytotoxicity of the probes. Confocal microscopy was then used to evaluate if AIE-ZnDPA could identify healthy early and late stage apoptotic cells treated with the widely used anticancer drug staurosporine (STS) and H_2O_2 as apoptotic inducers.[33,34] As shown in Figure S10 in the Supporting Information, the untreated live HeLa and HepG2 cells are not stained by AIE-ZnDPA or Alexa Fluor 488 annexin V. After treating the HeLa cells with 250 μM H_2O_2 for 6 h or 1 μM STS for 2 h to induce cell apoptosis, the cells were subsequently stained with AIE-ZnDPA and propidium iodide (PI). As shown in Figure 2A and

DOI: 10.1021/am508838z
ACS Appl. Mater. Interfaces 2015, 7, 4875−4882

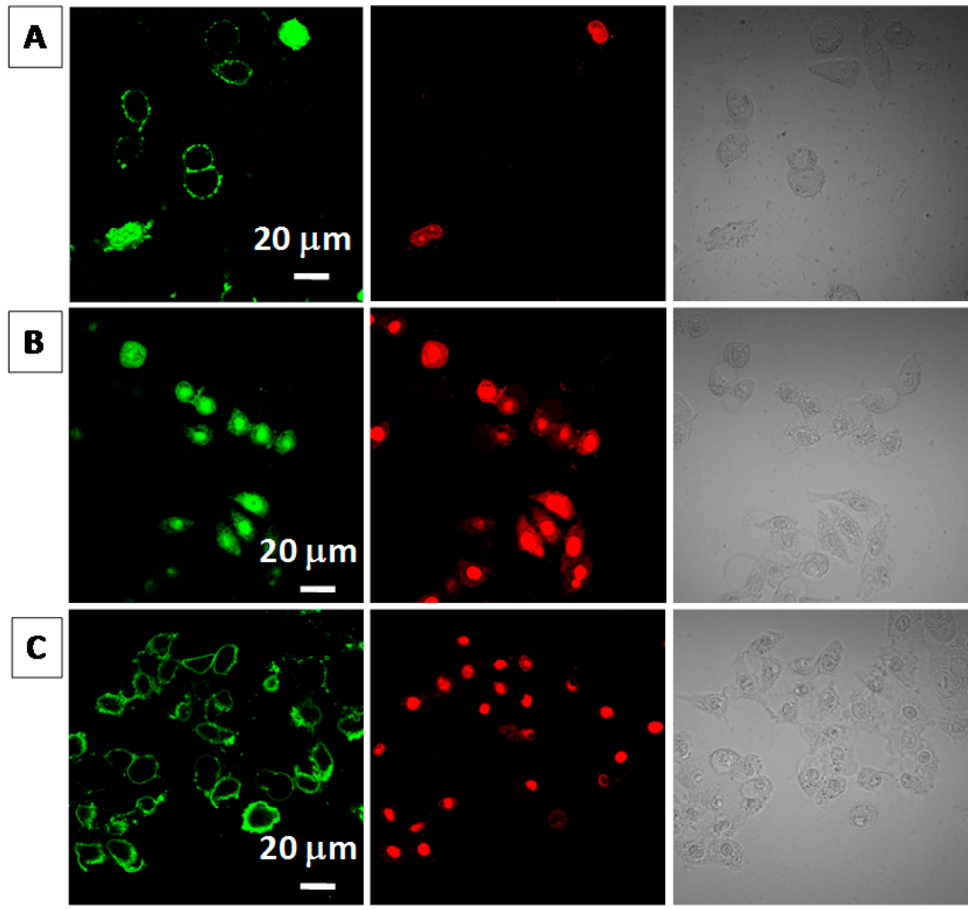

Figure 3. Confocal images of late stage apoptotic HeLa cells induced by 500 μM H_2O_2 for 6 h (A) or 2 μM staurosporine for 2 h (B), followed by incubation with 20 μM AIE-ZnDPA for 30 min at 37 °C and stained with 0.1 μg mL^{-1} propidium iodide for 5 min. (C) HeLa cells were treated with 2 μM staurosporine for 2 h, incubated with Alexa Fluor 488 annexin V for 30 min at 37 °C, and then stained with 0.1 μg mL^{-1} propidium iodide for 5 min. The red fluorescence originates from propidium iodide. All images share the same scale bar of 20 μm.

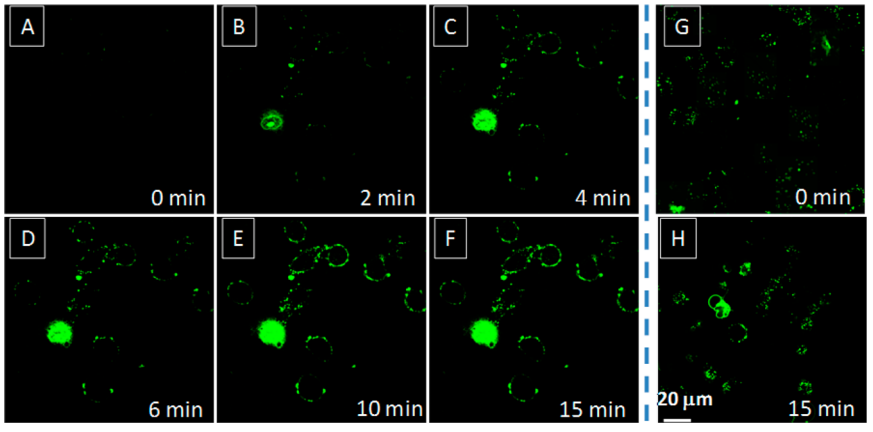

Figure 4. Real time fluorescence imaging of HeLa cells induced by 2 μM STS for 2 h, followed by the addition of 20 μM AIE-ZnDPA (A–F) or Alexa 488 annexin V (G–H). All images share the same scale bar of 20μm.

B, AIE-ZnDPA is able to anchor to the membrane of apoptotic cells after H_2O_2 or STS treatment. As PI can only stain dead cells, the absence of PI red fluorescence indicates that the cells are at the early stage of apoptosis. Parallel experiments were performed with Alexa Fluor 488 annexin V and PI. As shown in Figure 2C, Alexa Fluor 488 annexin V interacts with the externalized PS leading to membrane binding,[10,11] which is very similar to that of AIE-ZnDPA. It is worth noting that once the apoptotic cells were first stained with AIE-ZnDPA, subsequently staining with Alexa Fluor 488 annexin V would not yield any fluorescent signal from Alexa Fluor 488 (Supporting Information, Figure S11). This indicates that AIE-ZnDPA can block annexin V binding, which provides evidence that these two compounds compete for the same binding sites on the apoptotic cell surface.

Subsequently, we used 500 μM H_2O_2 for 6 h and 2 μM STS for 2 h to induce late stage cell apoptosis, and the results are shown in Figure 3. When the integrity of the cell membrane is

DOI: 10.1021/am508838z
ACS Appl. Mater. Interfaces 2015, 7, 4875–4882

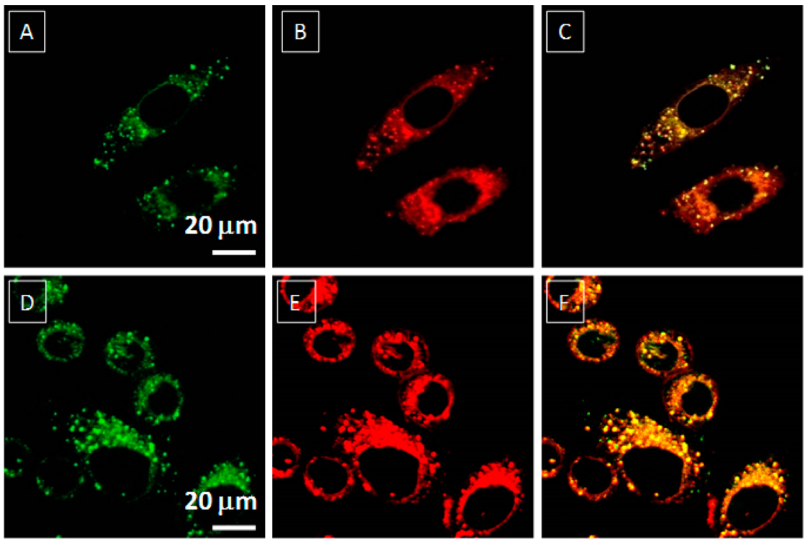

Figure 5. Confocal images of HeLa cells treated with PBS buffer (A–C) or 25 μM oleic acid for 6 h (D–F), followed by staining with 20 μM AIE-DPA for 30 min at 37 °C and costaining with 0.5 μM Nile Red for 5 min. AIE-DPA has Ex = 405 nm and a 510–560 nm band-pass filter. Nile Red has Ex = 543 nm and a 575–625 nm band-pass filter. All images share the same scale bar of 20 μm.

destroyed, the PI signal becomes obvious. The AIE-ZnDPA probe can enter into the cell nuclei and interact with negatively charged DNA to emit bright green fluorescence (Figure 3A and B). This is consistent with a previous report suggesting that tetraphenylethene-based zinc complexes exhibit high affinity for DNA.[35] However, for Alexa Fluor 488 annexin V, there is no difference between the staining of early and late stage apoptotic cells. This indicates the clear advantages of AIE-ZnDPA as a cell apoptosis probe, as it can differentiate early and late stages of live apoptotic cells under confocal microscopy. Moreover, because of the AIE characteristics of AIE-ZnDPA, its very low background fluorescence and high signal-to-noise ratio allows for real-time continuous monitoring of cell apoptosis without washing steps, which distinguishes the AIE probe from other existing fluorescent probes. As shown in Figure 4A–F, negligible background of AIE-ZnDPA is observed. As time elapses, the fluorescence intensity increases gradually to reache a maximum at 10 min. Commercial Alexa 488 annexin V, on the other hand, has a high background signal if washing steps are not performed (Figure 4G–H). These results indicate that the low background of the probe makes it suitable for real-time imaging of cell apoptosis.

To quantitatively detect cell apoptosis in a large population, flow cytometry was used to compare the utility of AIE-ZnDPA and Alexa Fluor 488 annexin V for identifying the apoptotic ratios of STS- and oxidant agent (H_2O_2)-induced HeLa cells. Cells treated with PBS were used as the control. The histograms in Figure S12 of the Supporting Information indicate that the fraction of apoptotic cells increases with the dose of STS and a nearly identical percentage of apoptotic cells was identified in each group when Alexa Fluor 488 annexin V was used. Similar results were also observed in the detection of H_2O_2-induced cell apoptosis (Supporting Information, Figure S13). Collectively, these results provide direct evidence that AIE-ZnDPA is a useful probe for the detection of cell apoptosis both qualitatively and quantitatively.

To understand the effect of zinc coordination in AIE-ZnDPA for apoptotic imaging, the precursor AIE-DPA without zinc coordination was also used for cell imaging studies. Interestingly, AIE-DPA enters live HeLa cells and specifically lights up the spherical lipid droplets, which overlap well with the Nile Red costain, a commercial dye used for lipid droplets imaging (Figure 5A–C). Lipid droplets are unique intracellular organelles surrounded by a monolayer of phospholipids that store neutral lipids for membrane synthesis and as an energy supply.[36] Abnormal accumulation of lipid droplets may be associated with several human pathologies.[37,38] This initial success of using AIE-DPA for lipid droplet staining has encouraged us to further explore its potential in imaging intracellular lipid droplet accumulation. Oleic acid can stimulate cells to produce lipid droplets, and upon treating HeLa cells with 25 μM oleic acid for 6 h, the amount of lipid droplets in the cells is significantly increased (Figure 5D–F). Similar trends are observed in HepG2 cells (Supporting Information, Figure S14). As it has already been reported that apoptosis can lead to the accumulation of cytoplasmic lipid droplets,[39,40] we further monitored the lipid droplets in apoptotic HeLa and HepG2 cells induced by STS. As shown in Figure S15 in the Supporting Information, AIE-DPA was observed to clearly stain intracellular lipid droplets. These results indicate that zinc coordination is essential for subcellular localization and the detection of cell apoptosis. Additionally, the photostability of AIE-DPA and AIE-ZnDPA was studied upon continuous laser scanning at 405 nm, and the fluorescent signal loss is less than 10% over ~8 min (Supporting Information, Figure S16), indicating good photostability of the probes.

3. CONCLUSIONS

In summary, we have developed the AIE- and ESIPT-based probe AIE-ZnDPA. The probe is weakly emissive in aqueous media, and it does not interact with healthy cells to yield fluorescence. However, similar to annexin V, AIE-ZnDPA can provide a clear green signal on the cell membrane to indicate early stages of cell apoptosis. More importantly, AIE-ZnDPA has the additional advantage of being able to differentiate early and late stage apoptosis by imaging the nuclei of late stage apoptotic cells. Differing from existing apoptosis probes with intrinsic fluorescence due to its low background fluorescence, AIE-ZnDPA offers the additional advantage of real-time continuous monitoring of cell apoptosis. Without zinc

DOI: 10.1021/am508838z
ACS Appl. Mater. Interfaces 2015, 7, 4875–4882

coordination, AIE-DPA enters both live and apoptotic cells and selectively accumulates in lipid droplets to light up its fluorescence. The AIE probe design strategy thus offers opportunities for subcellular localization-based biological monitoring.

4. EXPERIMENTAL SECTION

4.1. Materials. Anhydrous DMF, 2-hydroxybenzaldehyde, di(2-picolyl) amine, sodium carbonate, hydrazine monohydrate, ethanol, and methanol were all purchased from Aldrich. 1-palmitoyl-2-oleoyl-*sn*-glycero-3-phosphocholine (POPC) and 1-palmitoyl-2-oleoyl-*sn*-glycero-3-phosphoserine (POPS) were purchased from Sigma. 5-(Chloromethyl)-2-hydroxybenzaldehyde was synthesized according to procedures in the literature.[41]

Dulbecco's modified Eagle's medium (DMEM) was purchased from Invitrogen. Milli-Q water was supplied by Milli-Q Plus System (Millipore Corporation, Bedford, United States). Fetal bovine serum (FBS) and trypsin−EDTA solution were purchased from Gibco (Life Technologies, AG, Switzerland). Alexa Fluor 488 annexin V and Nile Red were purchased from Life Technologies. ssDNA was purchased from Sigma, and the sequence of ssDNA was 5′-GGGGGCGGGG-GCGGGGGCGG-3′. 3-(4,5-Dimethylthiazol-2-yl)-2,5-diphenyltetrazolium bromide (MTT), staurosporin, H_2O_2, propidium iodide solution, and other chemicals were all purchased from Sigma-Aldrich and used as received without further purification.

4.2. Characterization. UV−vis spectra were recorded on a Shimadzu UV-1700 spectrometer. Photoluminescence (PL) spectra were measured on a PerkinElmer LS-55 spectrometer. NMR spectra were collected on a Bruker Avance 400 NMR spectrometer. The high-resolution molecular mass was acquired using ion trap time-of-flight mass spectrometry. The chemical structures were also evaluated by Fourier-transform infrared spectroscopy (FTIR, Varian, Excalibur, USA). The fluorescence quantum yield was measured using quinine sulfate as the reference.

4.3. Fluorescence Measurements. Titration experiments were carried out at room temperature by adding different concentrations of DNA to 10 μM AIE-ZnDPA dissolved in distilled water. The PL spectra were then collected immediately. The fluorescence intensity of AIE-ZnDPA in Tris-HCl buffer, POPC, and POPS were also measured. Vesicle solutions (100 μM) of POPC and POPS were mixed at a 1:1 ratio before adding 10 μM AIE-ZnDPA. The PL spectra were measured immediately.

4.4. Cell Culture. HeLa human cervix carcinoma cells and HepG2 human liver hepatocellular carcinoma cells were cultured in DMEM containing 10% fetal bovine serum and 1% penicillin streptomycin at 37 °C in a humidified environment containing 5% CO_2.

4.5. Cell Viability Assay. A routine MTT assay was used for evaluatig the cytotoxicity of AIE-DPA and AIE-ZnDPA; the detailed procedure is described in the Supporting Information.

4.6. Cell Apoptosis Imaging. HeLa cells were cultured in chambers at 37 °C and grown for 18 h. The cells were treated with the anticancer drug staurosporin (1 and 2 μM) for 2 h and with hydrogen peroxide (250 and 500 μM) for 6 h. Then, the cells were divided into two groups, one for Alexa Fluor 488 annexin V staining and the other for AIE-ZnDPA staining. Alexa Fluor 488 annexin was used according to the manufacturer's protocol. Briefly, the cells were washed and resuspended in annexin binding buffer (10 mM HEPES−sodium salt, 2.5 mM $CaCl_2$, 140 mM NaCl, pH 7.4) containing 5 μL of Alexa Fluor 488 annexin V per 100 μL of buffer. The cells were incubated at room temperature for 15 min and further washed twice with PBS twice. Propidium iodide (0.1 μg mL^{-1}) was subsequently used to stain the nuclei of the cells for 5 min. For the competition assay, the HeLa cells were induced by 1 μM staurosporin for 2 h, stained with AIE-ZnDPA and then with Alexa Fluor 488 annexin V, or first stained with Alexa Fluor 488 annexin V followed by staining with AIE-ZnDPA. The cells were imaged immediately using a confocal laser scanning microscope (CLSM, Zeiss LSM 410, Jena, Germany). For annexin V detection, Ex = 488 nm, and Em = 510−560 nm. For propidium iodide imaging, Ex = 543 nm, and Em = 575−625 nm. In the case of AIE-ZnDPA staining, the cells were induced to undergo apoptotic processes as described above. Then, 20 μM AIE-ZnDPA was added to the cells and incubated for 15 min at room temperature. For AIE-ZnDPA, Ex = 405 nm, and Em = 510−560 nm.

4.7. Real-time Fluorescent Imaging. HeLa cells were cultured in chambers at 37 °C and grown for 18 h. The cells were treated with 2 μM staurosporine for 2 h followed by staining with 20 μM AIE-ZnDPA. The confocal images were taken at different times with excitation at 405 nm using 520/20 nm band-pass filter.

4.8. Flow Cytometry Analysis. HeLa cells at a density of 2×10^5 cells per well were seeded onto 6-well plates and grown for 18 h to achieve 80% confluence. Untreated cells were used as the control. The apoptotic cells were treated with 1 and 2 μM staurosporin for 2 h and 250 and 500 μM hydrogen peroxide for 6 h. The cells were then digested and collected. For annexin V staining, the collected cells were resuspended in 100 μL of annexin binding buffer containing 5 μL of the Alexa Fluor 488 annexin V. After incubating for 15 min at room temperature, 400 μL of PBS buffer was added to the cells and analyzed by flow cytometry (Dako Cytomation) using the Alexa 488 filter sets (λ_{ex} = 488 nm, 520/20 nm band-pass filter). For AIE-ZnDPA staining, the collected cells were resuspended in 100 μL of PBS with 20 μM AIE-ZnDPA for 15 min. Then, 400 μL of PBS buffer was added to the cells and analyzed by flow cytometry with excitation at 405 nm with 520/20 nm band-pass filter.

4.9. Lipid Droplet Imaging. HeLa and HepG2 cells were cultured in chambers at 37 °C and grown for 18 h. Untreated cells and cells treated with 25 μM oleic acid for 6 h or 1 μM staurosporine for 2 h were subsequently stained with 20 μM AIE-DPA for 30 min. Then, the cells were stained with 0.5 μM Nile Red for 5 min. The cells were imaged using a confocal microscope. For AIE-DPA, the excitation was 405 nm, and the emission filter was 510−560 nm; for Nile Red, the excitation was 543 nm, and the emission filter was 560 nm long pass.

4.10. Photostability Test. HeLa cells and HepG2 cells were treated with 2 μM STS for 2 h and stained with 20 μM AIE-ZnDPA at room temperature for 30 min. The CLSM images were recorded at different scan times under continuous laser scanning at an excitation wavelength of 405 nm (1% laser power), and the fluorescence intensity of each image was analyzed by Image Pro Plus software. The photostability of AIE-ZnDPA was indicated by the ratio of the fluorescence intensity after excitation for a designated time interval to its initial value as a function of the exposure time (n = 3).

■ ASSOCIATED CONTENT

Ⓢ Supporting Information

Synthetic generation of AIE-ZnDPA and AIE-DPA, characterization data of NMR, HMRS, and FTIR, cell viability, confocal imaging of untreated cells stained by AIE-ZnDPA and Alexa Fluor 488 annexin-V, flow cytometry, confocal imaging of AIE-DPA-stained HepG2 cells, and photostability analysis of AIE-DPA and AIE-ZnDPA. This material is available free of charge via the Internet at http://pubs.acs.org.

■ AUTHOR INFORMATION

Corresponding Author

*E-mail: cheliub@nus.edu.sg. Fax: (+65)6779-1936.

Author Contributions

⊥Q.H. and M.G. contributed equally to this work.

Notes

The authors declare no competing financial interest.

■ ACKNOWLEDGMENTS

We thank the Singapore National Research Foundation (R-279-000-390-281), SMART (R279-000-378-592), Ministry of Defence (R279-000-340-232), National University of Singapore (R279-000-415-112), and JCO (A*STAR, IMRE/14-8P1110) for financial support.

DOI: 10.1021/am508838z
ACS Appl. Mater. Interfaces 2015, 7, 4875−4882

REFERENCES

(1) Stavridi, F.; Karapanagiotou, E. M.; Syrigos, K. N. Targeted Therapeutic Approaches for Hormone-Refractory Prostate Cancer. *Cancer Treat. Rev.* **2010**, *36*, 122−130.

(2) Brindle, K. New Approaches for Imaging Tumour Responses to Treatment. *Nat. Rev. Cancer* **2008**, *8*, 94−107.

(3) Lee, B. W.; Olin, M. R.; Johnson, G. L.; Griffin, R. J. *In Vitro* and *in Vivo* Apoptosis Detection Using Membrane Permeant Fluorescent-Labeled Inhibitors of Caspases. *Methods Mol. Biol.* **2008**, *414*, 109−135.

(4) Nguyen, Q. D.; Smith, G.; Glaser, M.; Perumal, M.; Arstad, E.; Aboagye, E. O. Positron Emission Tomography Imaging of Drug-Induced Tumor Apoptosis with a Caspase-3/7 Specific [^{18}F]-Labeled Isatin Sulfonamide. *Proc. Natl. Acad. Sci. U.S.A.* **2009**, *106*, 16375−16380.

(5) Wu, Y.; Xing, D.; Luo, S.; Tang, Y.; Chen, Q. Detection of Caspase-3 Activation in Single Cells by Fluorescence Resonance Energy Transfer During Photodynamic Therapy Induced Apoptosis. *Cancer Lett.* **2006**, *235*, 239−247.

(6) Eldadah, B. A.; Yakovlev, A. G.; Faden, A. I. A New Approach for the Electrophoretic Detection of Apoptosis. *Nucleic Acids Res.* **1996**, *24*, 4092−4093.

(7) Walker, P. R.; Leblanc, J.; Smith, B.; Pandey, S.; Sikorska, M. Detection of DNA Fragmentation and Endonucleases in Apoptosis. *Methods* **1999**, *17*, 329−338.

(8) White, M. K.; Cinti, C. A Morphologic Approach to Detect Apoptosis Based on Electron Microscopy. *Methods Mol. Biol.* **2004**, *285*, 105−111.

(9) Schlegel, R. A.; Williamson, P. Phosphatidylserine, a Death Knell. *Cell Death Differ.* **2001**, *8*, 551−63.

(10) Plasier, B.; Lloyd, D. R.; Paul, G. C.; Thomas, C. R.; Al-Rubeai, M. Automatic Image Analysis for Quantification of Apoptosis in Animal Cell Culture by Annexin-V Affinity Assay. *J. Immunol. Methods* **1999**, *229*, 81−95.

(11) Jung, K. H.; Lee, J. H.; Park, J. W.; Paik, J. Y.; Quach, C. H.; Lee, E. J.; Lee, K. H. Annexin V Imaging Detects Diabetes-Accelerated Apoptosis and Monitors the Efficacy of Benfotiamine Treatment in Ischemic Limbs of Mice. *Mol. Imaging* **2014**, *13*, 1−7.

(12) Williamson, P.; van den Eijnde, S.; Schlegel, R. A. Phosphatidylserine Exposure and Phagocytosis of Apoptotic Cells. *Methods Cell Biol.* **2001**, *66*, 339−364.

(13) Koulov, A. V.; Stucker, K. A.; Lakshmi, C.; Robinson, J. P.; Smith, B. D. Detection of Apoptotic Cells Using a Synthetic Fluorescent Sensor for Membrane Surfaces That Contain Phosphatidylserine. *Cell Death Differ.* **2003**, *10*, 1357−1359.

(14) Kwong, J. M.; Hoang, C.; Dukes, R. T.; Yee, R. W.; Gray, B. D.; Pak, K. Y.; Caprioli, J. Bis(zinc-dipicolylamine), Zn-DPA, a New Marker for Apoptosis. *Invest. Ophthalmol. Visual Sci.* **2014**, *55*, 4913−4921.

(15) Hanshaw, R. G.; Lakshmi, C.; Lambert, T. N.; Johnson, J. R.; Smith, B. D. Fluorescent Detection of Apoptotic Cells by Using Zinc Coordination Complexes with a Selective Affinity for Membrane Surfaces Enriched with Phosphatidylserine. *ChemBioChem* **2005**, *6*, 2214−2220.

(16) O'Neil, E. J.; Jiang, H.; Smith, B. D. Effect of Bridging Anions on the Structure and Stability of Phenoxide Bridged Zinc Dipicolylamine Coordination Complexes. *Supramol. Chem.* **2013**, *25*, 315−322.

(17) Ding, D.; Li, K.; Liu, B.; Tang, B. Z. Bioprobes Based on AIE Fluorogens. *Acc. Chem. Res.* **2013**, *46*, 2441−2453.

(18) Shi, H.; Kwok, R. T.; Liu, J.; Xing, B.; Tang, B. Z.; Liu, B. Real-Time Monitoring of Cell Apoptosis and Drug Screening Using Fluorescent Light-Up Probe with Aggregation-Induced Emission Characteristics. *J. Am. Chem. Soc.* **2012**, *134*, 17972−17981.

(19) Zhao, J.; Yang, D.; Zhao, Y.; Yang, X. J.; Wang, Y. Y.; Wu, B. Anion-Coordination-Induced Turn-On Fluorescence of an Oligourea-Functionalized Tetraphenylethene in a Wide Concentration Range. *Angew. Chem., Int. Ed.* **2014**, *53*, 6632−6636.

(20) Liu, M.; Zhang, X.; Yang, B.; Liu, L.; Deng, F.; Wei, Y. Polylysine Crosslinked AIE Dye Based Fluorescent Organic Nanoparticles for Biological Imaging Applications. *Macromol. Biosci.* **2014**, *14*, 1260−1267.

(21) Yuan, Y.; Kwok, R. T.; Tang, B. Z.; Liu, B. Targeted Theranostic Platinum(IV) Prodrug with a Built-in Aggregation-Induced Emission Light-Up Apoptosis Sensor for Noninvasive Early Evaluation of its Therapeutic Responses in Situ. *J. Am. Chem. Soc.* **2014**, *136*, 2546−2554.

(22) Hu, F.; Huang, Y.; Zhang, G.; Zhao, R.; Yang, H.; Zhang, D. Targeted Bioimaging and Photodynamic Therapy of Cancer Cells with an Activatable Red Fluorescent Bioprobe. *Anal. Chem.* **2014**, *86*, 7987−7995.

(23) Li, C.; Wu, T.; Hong, C.; Zhang, G.; Liu, S. A General Strategy to Construct Fluorogenic Probes from Charge-Generation Polymers (CGPs) and AIE-Active Fluorogens Through Triggered Complexation. *Angew. Chem., Int. Ed.* **2012**, *51*, 455−459.

(24) Li, K.; Liu, B. Polymer-Encapsulated Organic Nanoparticles for Fluorescence and Photoacoustic Imaging. *Chem. Soc. Rev.* **2014**, *43*, 6570−6597.

(25) Zhang, X.; Zhang, X.; Yang, B.; Yang, Y.; Wei, Y. Renewable Itaconic Acid Based Cross-Linked Fluorescent Polymeric Nanoparticles for Cell Imaging. *Polym. Chem.* **2014**, 5885−5889.

(26) Li, H.; Zhang, X.; Yang, B.; Yang, Y.; Huang, Z.; Wei, Y. Zwitterionic Red Fluorescent Polymeric Nanoparticles for Cell Imaging. *Macromol. Biosci.* **2014**, *14*, 1361−1367.

(27) Hong, Y.; Lam, J. W.; Tang, B. Z. Aggregation-Induced Emission. *Chem. Soc. Rev.* **2011**, *40*, 5361−5388.

(28) Gao, M.; Sim, C. K.; Leung, C. W.; Hu, Q.; Feng, G.; Xu, F.; Tang, B. Z.; Liu, B. A Fluorescent Light-Up Probe with AIE Characteristics for Specific Mitochondrial Imaging to Identify Differentiating Brown Adipose Cells. *Chem. Commun. (Cambridge, U.K.)* **2014**, *50*, 8312−8315.

(29) Song, Z.; Kwok, R. T.; Zhao, E.; He, Z.; Hong, Y.; Lam, J. W.; Liu, B.; Tang, B. Z. A Ratiometric Fluorescent Probe Based on ESIPT and AIE Processes for Alkaline Phosphatase Activity Assay and Visualization in Living Cells. *ACS Appl. Mater. Interfaces* **2014**, *6*, 17245−17254.

(30) Tang, W.; Xiang, Y.; Tong, A. Salicylaldehyde Azines as Fluorophores of Aggregation-Induced Emission Enhancement Characteristics. *J. Org. Chem.* **2009**, *74*, 2163−2166.

(31) Li, N.; Tang, W.; Xiang, Y.; Tong, A.; Jin, P.; Ju, Y. Fluorescent Salicylaldehyde Hydrazone as Selective Chemosensor for Zn^{2+} in Aqueous Ethanol: A Ratiometric Approach. *Luminescence* **2010**, *25*, 445−451.

(32) Li, K.; Wang, X.; Tong, A. A "Turn-On" Fluorescent Chemosensor for Zinc Ion with Facile Synthesis and Application in Live Cell Imaging. *Anal. Chim. Acta* **2013**, *776*, 69−73.

(33) Bauer, C.; Bauder-Wuest, U.; Mier, W.; Haberkorn, U.; Eisenhut, M. ^{131}I-Labeled Peptides as Caspase Substrates for Apoptosis Imaging. *J. Nucl. Med.* **2005**, *46*, 1066−1074.

(34) Guo, Z.; Kim, G. H.; Yoon, J.; Shin, I. Synthesis of a Highly Zn^{2+}-Selective Cyanine-Based Probe and Its Use for Tracing Endogenous Zinc Ions in Cells and Organisms. *Nat. Protoc.* **2014**, *9*, 1245−1254.

(35) Zhu, Z.; Xu, L.; Li, H.; Zhou, X.; Qin, J.; Yang, C. A Tetraphenylethene-Based Zinc Complex as a Sensitive DNA Probe by Coordination Interaction. *Chem. Commun. (Cambridge, U.K.)* **2014**, *50*, 7060−7062.

(36) Wooding, F. B. Lipid Droplet Secretion by the Rabbit Harderian Gland. *J. Ultrastruct. Res.* **1980**, *71*, 68−78.

(37) Krahmer, N.; Farese, R. V., Jr.; Walther, T. C. Balancing the Fat: Lipid Droplets and Human Disease. *EMBO Mol. Med.* **2013**, *5*, 905−915.

(38) Przybytkowski, E.; Behrendt, M.; Dubois, D.; Maysinger, D. Nanoparticles Can Induce Changes in the Intracellular Metabolism of Lipids without Compromising Cellular Viability. *FEBS J.* **2009**, *276*, 6204−6217.

(39) Yamanaka, K.; Urano, Y.; Takabe, W.; Saito, Y.; Noguchi, N. Induction of Apoptosis and Necroptosis by 24(S)-Hydroxycholesterol

DOI: 10.1021/am508838z
ACS Appl. Mater. Interfaces 2015, 7, 4875−4882

is Dependent on Activity of Acyl-CoA:Cholesterol Acyltransferase 1. *Cell Death Dis.* **2014**, *5*, e990-1−e990-9.
(40) Boren, J.; Brindle, K. M. Apoptosis-Induced Mitochondrial Dysfunction Causes Cytoplasmic Lipid Droplet Formation. *Cell Death Differ.* **2012**, *19*, 1561−1570.
(41) Cort, A. D.; Mandolini, L.; Pasquini, C.; Schiaffino, L. A Novel Ditopic Zinc-Salophen Macrocycle: A Potential Two-Stationed Wheel for [2]-Pseudorotaxanes. *Org. Biomol. Chem.* **2006**, *4*, 4543−4546.

DOI: 10.1021/am508838z
ACS Appl. Mater. Interfaces 2015, 7, 4875−4882